ISSN : 2320-2882



## INTERNATIONAL JOURNAL OF CREATIVE **RESEARCH THOUGHTS (IJCRT)**

An International Open Access, Peer-reviewed, Refereed Journal

# Zirconium (Zr<sup>4+</sup>) Substituted Batio<sub>3</sub>: A Study Of Structural, Dielectric And Optical Characteristics

<sup>1</sup>Arpita Patel, <sup>2</sup>Rajesh Kumar Katare

<sup>1</sup>Research Scholar, Department of Physics, SAGE University, Indore (M.P.) 452001-India <sup>2</sup>Asst. Professor, Department of Physics, SAGE University, Indore (M.P.) 452001-India

**Abstract:** The structural and electrical characteristics of Zirconium (Zr) doped BaTiO<sub>3</sub> is discussed here. Taking into the consideration the excellent dielectric and ferroelectric properties of BaTi<sub>0.9</sub>Zr<sub>0.1</sub>O<sub>3</sub>, it is the extensively studied material till date. It is currently used in many different fields, such as field-effect transistors, multilayer capacitors, actuators, transducers, dynamic random-access memory, and electrooptical devices. Taking into the consideration these applications, Zr has been selected as the substituent for BaTiO<sub>3</sub> (BaTi<sub>0.9</sub>Zr<sub>0.1</sub>O<sub>3</sub>) to modify its physical properties. Hereby, we report synthesis of BaTi<sub>0.9</sub>Zr<sub>0.1</sub>O<sub>3</sub> using solid state route and investigated its crystallization via XRD and also emphasized on its dielectric and impedance characteristics. XRD analysis reveals tetragonal crystal structure of the synthesized sample. Lattice structure was further verified by the analysis of Raman inelastic scattering. The response of dielectric properties to the applied ac field frequency infers the sample to inherit higher dielectric permittivity with relatively. Conduction mechanism was investigated using electric modulus and impedance studies. Impedance study reveals non-ideal Debye-like nature of the ceramic. The optical band gap of the sample was estimated to be 3.2eV determined from UV-Vis Diffuse reflectance spectroscopy in terms of Tuac's plot.

Keywords: Perovskites; Ferroelectrics, Structure; Dielectric Properties; Optical Bandgap.

## I. Introduction

An environmentally acceptable dielectric and ferroelectric material, barium titanate (BaTiO<sub>3</sub>) performs comparably to several Pb-based electro-ceramics. It is widely used in the production of electronic gadgets such as piezoelectric transducers, micro-electro mechanical systems (MEMs), dynamic random access memories (DRAM) etc., By virtue of its ubiquitous dielectric nature, it is readily exploited in the fields of PTC thermistors, and multilayer ceramic capacitors (MLCC) and so on [1-4].

It is well established fact that as the particle size reduces in tetragonal phase, the lattice constant (c/a) ratio lowers as well. Consequently, the dielectric and ferroelectric characteristics of the ceramics can be altered by adjusting the grain size. It was discovered that as grain size reduces, dielectric permittivity increases [5,6]. One method of controlling the growth of ceramic grains is to create ceramic pellets using nanopowders as a source. So, it is important to regulate the grain size of ceramic layers to make it sufficiently small. For practical applications, the regulation of T<sub>c</sub> in ferroelectric materials is crucial since the permanent polarization vanishes above the Curie temperature. Ba(Zr<sub>x</sub>Ti<sub>1-x</sub>)O<sub>3</sub> (BZT) is employed recently for the preparation of ceramic capacitors due to Zr<sup>4+</sup> having greater chemical stability than Ti<sup>4+</sup>. Furthermore, it has been discovered that Zr-substitution at Ti-site effectively lowers the Curie temperature and exhibits a number of intriguing characteristics in the dielectric nature of BaTiO<sub>3</sub> ceramics [5-9].

The solid solution of BaTiO<sub>3</sub> and BaZrO<sub>3</sub> is a well established material composition with significant dielectric impacts that is used in multilayer capacitors. Zirconium is added to BaTiO<sub>3</sub> ceramic to increase its high permittivity, which satisfies the Z5U MLC standard [10-12]. The Zr<sup>4+</sup> ion (72 Å) increases the perovskite lattice due to its higher ionic radius and chemical stability over the Ti<sup>4+</sup> (0.60 Å) ion. As a result, the dielectric behavior of BZT material displays a number of intriguing characteristics. With increasing Zr content in BZT ceramic, there is a significant change in the nature of ferroelectric phase transitions at the Curie temperature (T<sub>c</sub>) [11-13].

Titanates were studied for many uses using a variety of synthesis and doping techniques. Because of the high temperatures required for solid-state processes, the typical method of synthesizing ceramic powders favors the production of hard agglomerates. Based on this character, several techniques were developed recently to replace the traditional one, producing barium titanate that is less agglomerated and in finer powder. It was investigated how to modify the conventional solid-state reaction approach to lower the synthesis temperature and produce powder without hard agglomeration [13,15]. In this work, a solid-state process was used to produce zirconium doped barium titanate.

#### 2 EXPERIMENTAL DETAILS

#### 2.1 SAMPLE SYNTHESIS

Zirconium titanate (BaTi<sub>0.9</sub>Zr<sub>0.1</sub>O<sub>3</sub>) sample was synthesized solid state reaction by double calcinations route [16]. Without further purification, the raw materials viz BaCO<sub>3</sub>, ZrO<sub>2</sub>, TiO<sub>2</sub> were used. The materials were weighed in stoichiometric ration and mixed with mechanical grinding using agate mortar-pestle. Acetone was added to the mixture while grinding for proper dispersion. Grinding for 4h and 3h was followed by calcinations at 1000 °C and 1100°C at 5h respectively. The final calcined mixture was transferred into pellets under hydraulic press at a pressure of 5tonnes per inch square. The pellet was sintered at1200 °C for 5h to form a compact material. A smooth conducting surface for proper electrical contacts was formed on the pellets by silver paste polishing.

#### 2.2 EXPERIMENTATION

We used X-ray diffraction (XRD) analysis to detect phase formation and establish the structure of the synthesized BaTiO<sub>3</sub> sample. The experiment was conducted using diffractometer whose model, name and specifications are mentioned in section 4.3.2. The samples were subjected to dielectric tests with a Precision LCR meter (Model E4980A) from Keysight Technologies (2Hz-2MHz). To estimate the bandgap of the material, UV-Vis spectroscopy was employed and the spectrometer was Perkin Elmer, USA Model: Lambda 950 spectometer.

#### 3 RESULTS AND DISCUSSIONS

#### 3.1 STRUCTURAL ANALYSIS

XRD diffractogram of BaTi<sub>0.9</sub>Zr<sub>0.1</sub>O<sub>3</sub> is shown as Figure 1. It is obvious that the analysis that sample is crystalline. Furthermore analysis reveals tetragonal structure [44] of the sample. The sharp and intense reflections reveal that the particles are very crystalline arising from high temperature treatment whereas the narrowness of the diffraction peaks indicates that the average crystallite size is very large. The particle size calculated using Debye-Scherer's formula is 98nm.

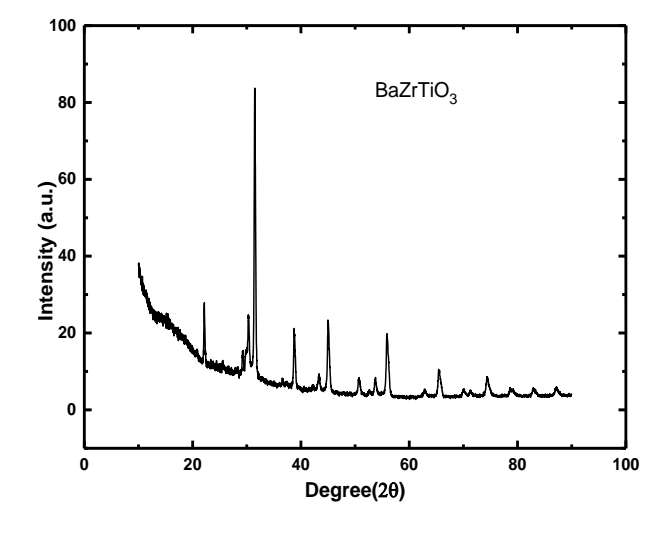


**Figure 1:** X-ray diffraction pattern of BaTi<sub>0.9</sub>Zr<sub>0.1</sub>O<sub>3</sub> ceramic material

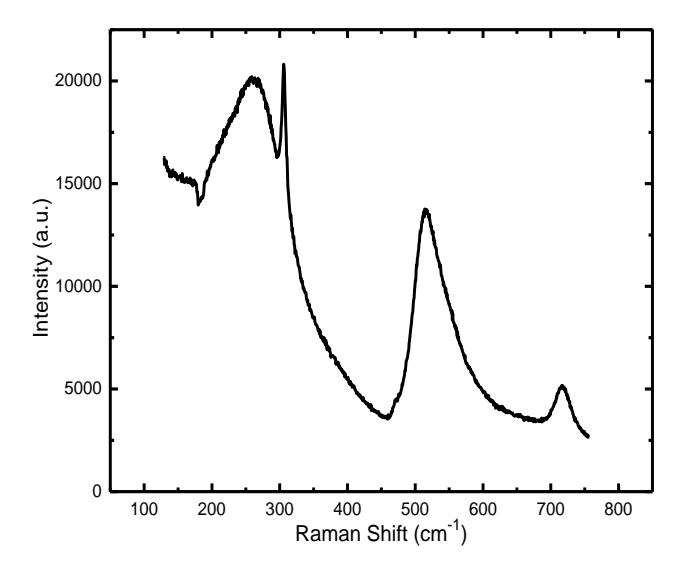


Figure 2: Raman spectrum of BaTi<sub>0.9</sub>Zr<sub>0.1</sub>O<sub>3</sub> material

#### 3.2: RAMAN INELASTIC SCATTERING

After being captured and plotted, the Raman spectrum is shown in Figure 2. The spectrum analysis reveals some distinctive absorption peaks that indicate the tetragonal phase development. The Raman spectrum of the Zr doped BaTiO<sub>3</sub> (BaTi<sub>0.9</sub>Zr<sub>0.1</sub>O<sub>3</sub>) system, recorded at room temperature, is displayed in Figure 2. A broad peak at around 715 cm<sup>-1</sup> and a small shoulder peak at about 310 cm<sup>-1</sup> are seen in all of Fig. 3's spectra together with additional peaks; these peaks are indicative of structural tetragonality (P4mm symmetry). The observed anti-resonance effect at 183 cm<sup>-1</sup> as an interference feature to a connection between the broad A1(TO2) and sharp A1 (TO1) modes. Thus the tetragonal structure revealed from the Raman spectrum for BZT sample is in agreement with the XRD results. [17,18]

#### 3.3: DIELECTRIC STUDIES

## 3.3.1 PERMITTIVITY AND DISSIPATION

The dielectric permittivity of BaTi<sub>0.9</sub>Zr<sub>0.1</sub>O<sub>3</sub>, as shown in Figure 3, follows the typical pattern of declining as field values rise. The polarization of space charges is responsible for the increased dielectric permittivity value at low field levels. The Maxwell-Wagner Model provides an explanation for the lower dielectric permittivity at higher frequencies and the larger value at lower frequencies. Actually, polarization comes into existence when charges pile at grain insulating boundaries. Higher the piling, greater is the polarization that diminishes with increase in the field value [19-21].

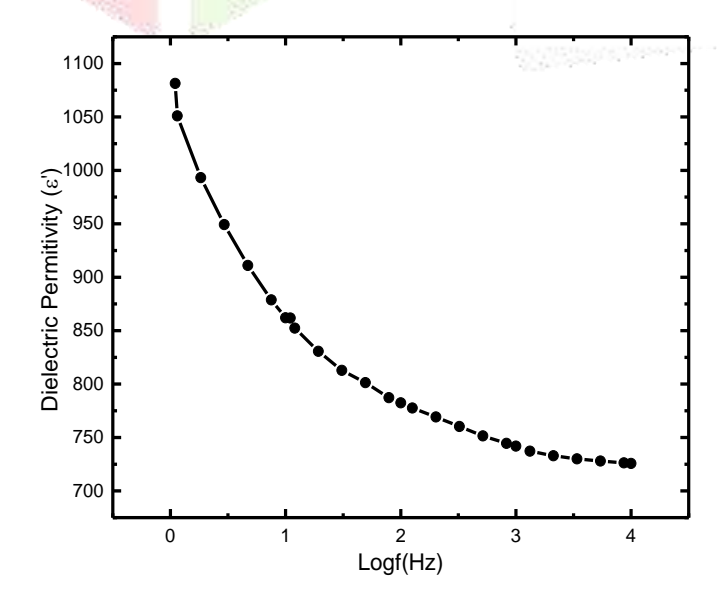


**Figure 3**: Dielectric permittivity of BaTi<sub>0.9</sub>Zr<sub>0.1</sub>O<sub>3</sub> ceramic material

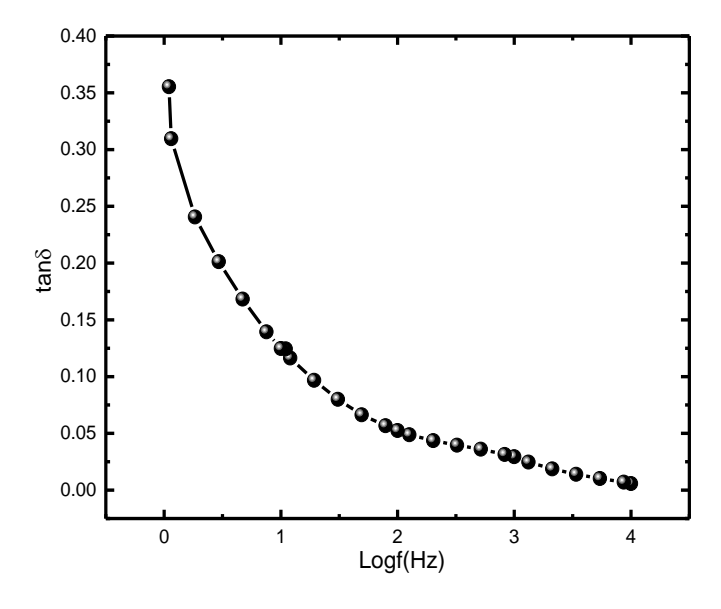


Figure 4: Dielectric loss of BaTi<sub>0.9</sub>Zr<sub>0.1</sub>O<sub>3</sub> ceramic material

Similar to the dielectric constant of dielectric materials, the dielectric loss in Figure 4 first shows a declining trend as field values increase in response to the field. The lattice flaws and contaminants cause the dielectric loss. The dielectric loss reduces at high frequencies as a result of domain wall motion suppression. It is discovered that at lower frequencies, the dielectric loss is greatest. This happens when the hopping frequency of electrons between various ionic sites approaches the frequency of the applied ac field. Furthermore, dielectric loss is believed to arise from impurities and structural inhomogeneities that cause the polarization to lag behind the applied alternating field [20-22].

## 3.4 CONDUCTIVITY $(\Sigma_{AC})$

It was discovered that the ac conductivity of the BaTi<sub>0.9</sub>Zr<sub>0.1</sub>O<sub>3</sub> ceramic material shown in Figure 5 is constant at first and increases as frequency is increased further. This nature is thought to arise from charge carriers hopping between several localized states as a result of an increase in applied field. As a consequence, there is an improvement in electron immigration, which raises conductivity at higher frequencies. The initial lack of response to the applied field suggests that there is no ac conductivity, and any current detected is due to the dc conductivity of the material under observation. Generally, Jonscher's law holds the conductivity in the materials. The law defines the region corresponding to low applied frequency values which does not respond the applied field abd the region that briefs about ac conductivity [19-24].

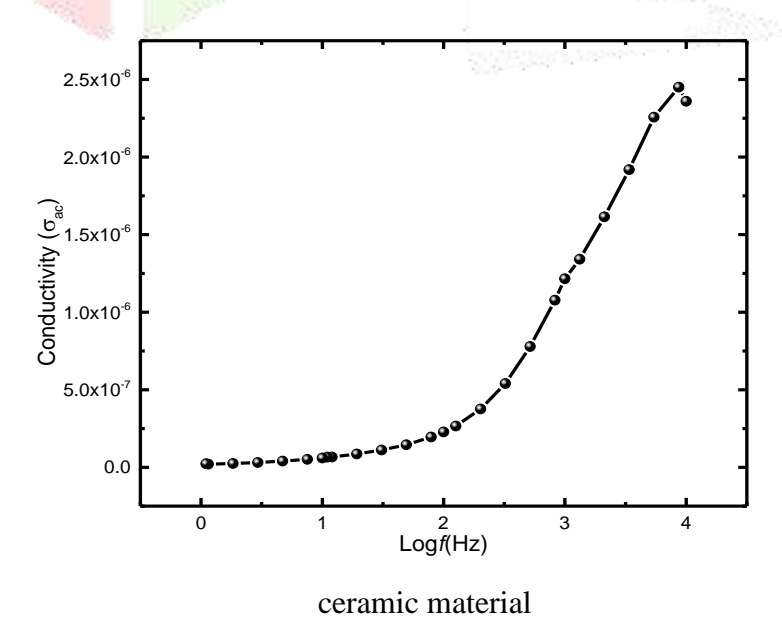


Figure 5: Dielectric

loss of BaTi<sub>0.9</sub>Zr<sub>0.1</sub>O<sub>3</sub>

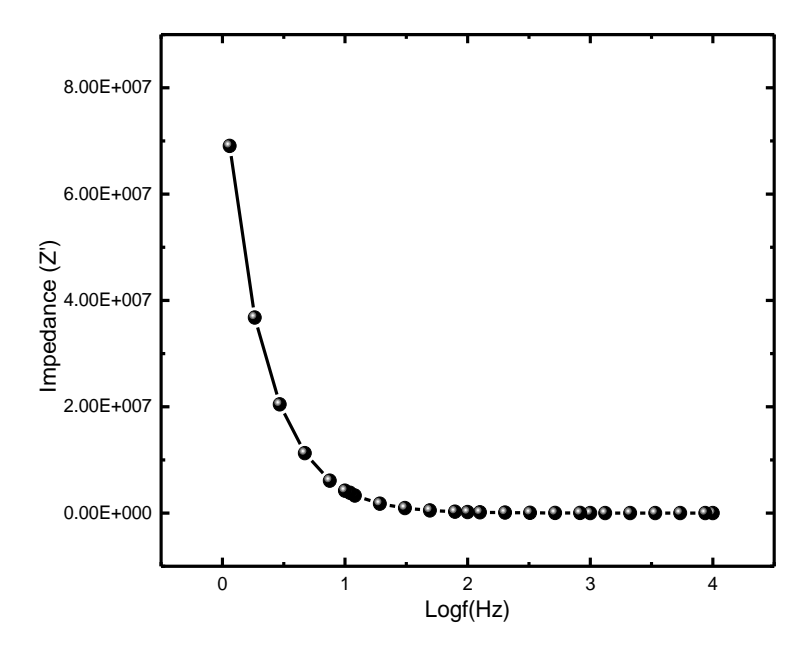


Figure 6: Impedance (Z', real of BaTi<sub>0.9</sub>Zr<sub>0.1</sub>O<sub>3</sub> ceramic material.

#### 3.5 **IMPEDANCE ANALYSIS**

Impedance spectroscopy enables us to determine the various contributions to dielectric constant, such as grain, grain boundaries and electrode effect. Impedance of dielectric materials is a measure of how a material responds to an applied electric field of a fixed or changing frequency. This is studied using dielectric spectroscopy (DS) or impedance spectroscopy, which is also known as electrochemical impedance spectroscopy. The variation of the real component of impedance (Z') with frequency is depicted in Figure 6. The actual part of the impedance monotonically decreases above 10 kHz and reaches a constant value at higher frequencies. It is brought on by either a constant lowering of barrier properties or the release of space charge [24-26].

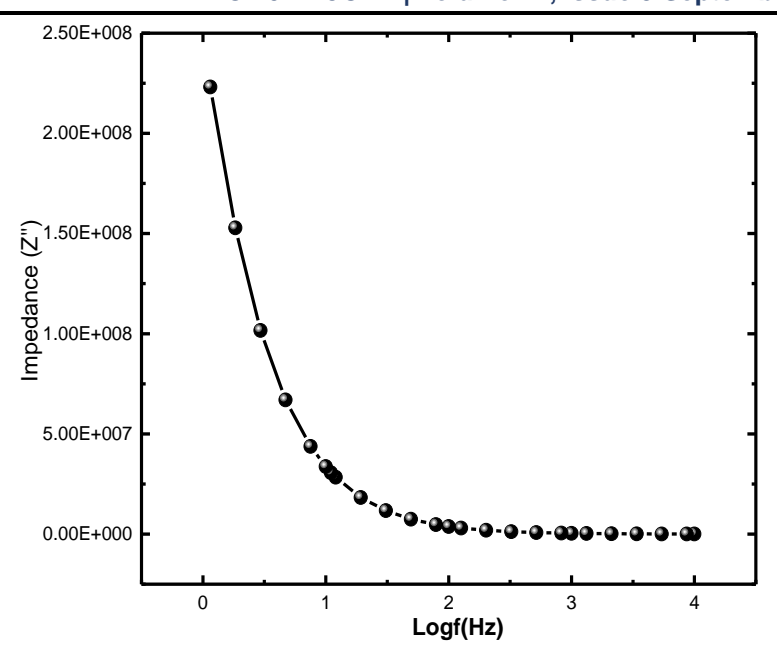


Figure 7: Impedance (Z", Img) of BaTi<sub>0.9</sub>Zr<sub>0.1</sub>O<sub>3</sub> ceramic material

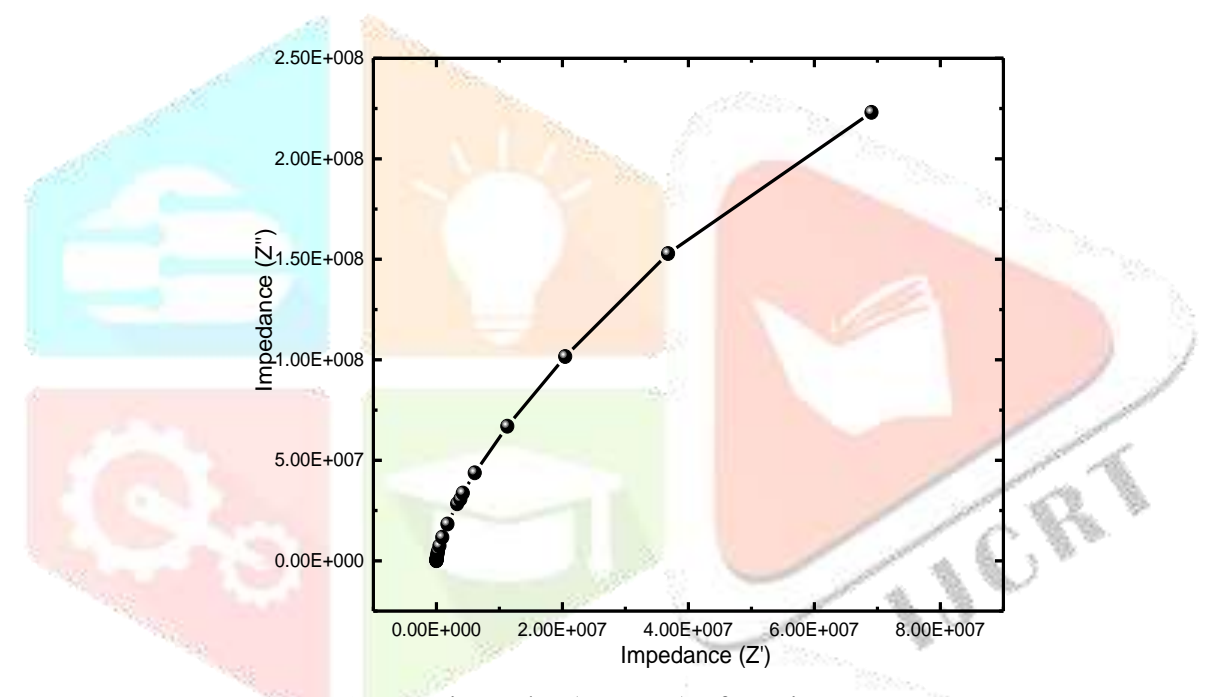


Figure 8: Nyquist's plot (Z' vs Z") of BaTi<sub>0.9</sub>Zr<sub>0.1</sub>O<sub>3</sub> ceramic material

Figure 7 displays the imaginary component of impedance (Z"), which is dependent on frequency. The Z" variance represents the distribution of relaxation time. Electrons and immobile charges are the main relaxation species at room temperature. Hopping of oxygen ion vacancies among localized site is believed to give rise to electrical conductivity [25-28]. The impedance characterization is important to emphasize on conduction mechanism. Figure 8 displays the impedance characteristics of the of BaTi<sub>0.9</sub>Zr<sub>0.1</sub>O<sub>3</sub> sample. An impedance spectrum is a Nyquist's diagram that shows the imaginary (Z") versus real (Z') part of the impedance. Here, the sample under study displays only one semi-circular arc, suggesting that the impedance is mainly caused by the interior of the grain. Furthermore, it seems that center of the semicircle is located well below the Z' axis, suggesting non-Debye behavior [29-31].

#### **OPTICAL BANDGAP** 3.6

Materials based on BaTO<sub>3</sub> are indispensable or optical device applications. To adjust material for a better performance, optical bandgap is an important tool. To estimate the band gap, UV-Vis diffuse reflectance spectra has been recorded. The obtained data has been transferred according to Kubelka-Munk Function viz.  $[F(R)hv]^n$ . Tauc's plot for BaTi<sub>0.9</sub>Zr<sub>0.1</sub>O<sub>3</sub> perovskite is shown in Figure 9. For n = 2, a straight transition, the Kubelka-Munk function [F(R)hv]<sup>n</sup> was displayed as a function of energy (hv). The line drawn along the sharp edge intersects the energy axis at 3.2, showing that the energy bandgap of BaTi<sub>0.9</sub>Zr<sub>0.1</sub>O<sub>3</sub> is less than the bandgap value of BaTiO<sub>3</sub> at roughly 3.2 eV. The band gap value determined is relatively less than pristine BaTiO<sub>3</sub> perovskite material. The reduced value of optical band gap is attributed to the impurities, defects and shrinks in the bands. This bandgap value is tunable for photo-catalysts and other photoelectronic device applications [29,32,33].

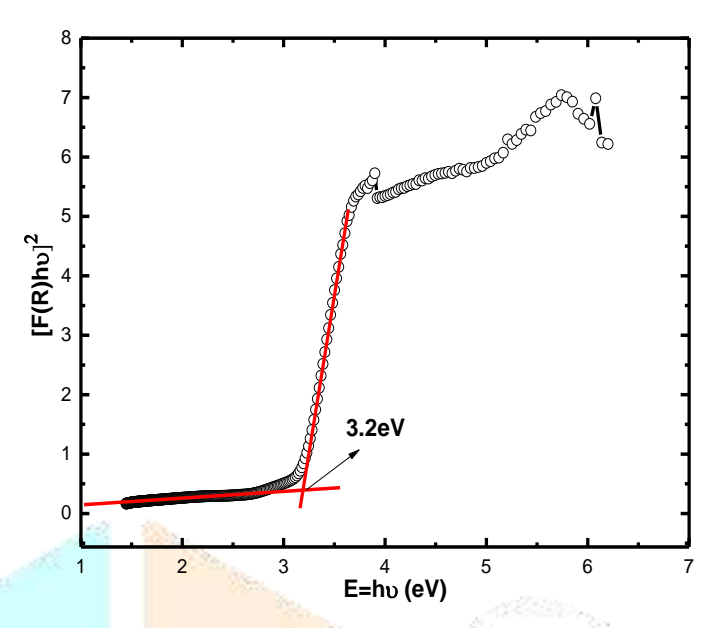


Figure 9: Tuac's plot of BaTi<sub>0.9</sub>Zr<sub>0.1</sub>O<sub>3</sub>

#### 4. CONCLUSIONS

The titanate of the type BaTi<sub>0.9</sub>Zr<sub>0.1</sub>O<sub>3</sub> is found to be the intriguing ferroelectric material. Here this material was effectively synthesized by solid state route at high temperature and the method is called the double calcination solid state reaction route. The sample was studied for structural, optical and dielectric properties. The structural studies carried via X-ray diffraction technique and Raman inelastic scattering spectroscopic method. The analysis of the XRD spectrum has revealed tetragonal structure with space group P4mm whereas acquired lattice structure was verified from the fingerprint Raman modes. The dielectric propertied were technologically worth from high dielectric permittivity and low loss value point of view. Impedance studies revealed near insulating nature and non-Debye feature exhibited by the sample. The optical band gap estimated to be 3.2eV is feasible for device applications.

#### ACKNOWLEDGMENT

Authors acknowledge Department of physics, SAGE University for encouraging carrying out this project. Further, Dept. of Physics in general and Dr. Netram Kaurav sir in particular for laboratory and characterization facility.

#### REFERENCES

- [1] P. Setasuwon, N. Vaneesorn, S. Kijamnajsuk and A. Thanaboonsombut: Science and Technology of AdvancedMaterials, 6 (2005) 278.
- R. Zuo, C. Ye, X. Fang and J. Li: Journal of the European Ceramic Society 28 (2008) 871. [2]
- W. Chaisan, R. Yimnirun and Ananta: Ceramics International, 35 (2009) 173
- [4] A.E. Souza, R.A. Silva, G.T.A. Santos, M.L. Moreira, D.P. Volanti, S.R. Teixeira and E. Longo: Chemical Physics Letters 488 (2010) 54.
- [5] M. Aghayan, A. K. Zak, M. Behdani, A. M. Hashim, Ceramics International, 40 (2014) 16141-16146
- M. Reda, S. I. El-Dek, & M. M. Arman, J Mater Sci: Mater Electron 33 (2022) 16753–16776 [6]
- B. G. Glos, K. Bormanis, D. Sitko, Ferroelectrics 417(1) (2011) 118-123 [7]
- [8] S. Mahajan, O. P. Thakur, C. Prakash and K Sreenivas, Bull. Mater. Sci., 34 (2011) 1483–1489.
- [9] I. Rivera, A. Kumar, N. Ortega, R.S. Katiyar, S. Lushnikov, Solid State Commun. 149(3–4) (2009) 172– 176
- [10] X. G. Tang, K. H. Chew and H. L. W. Chan, Acta Mater. 52 (2004) 5177
- [11] T. Maiti, R. Guo and A. S. Bhalla Appl. Phys. Lett. 100 (2006) 114109
- [12] T. Maiti, R. Guo and A. S. Bhalla Appl. Phys. Lett. 89 (2006) 122909
- [13] I. Zouari et. al., J. Electron. Mater. 46(7) (2017).4662–4669

- [14] P. Setasuwon, N. Vaneesorn, S. Kijamnajsuk and A. Thanaboonsombut: Science and Technology of Advanced Materials, 6 (2005) 278.
- [15] P. Nimmanpipug, A. Saelor, L. Srisombat, V.S. Lee and Y. Laosiritaworn: Ceramics International 39 (2013) S293.
- [16] A. A. Kholodkova, M. N. Danchevskaya, Yu.D. Ivakin, A. D. Smirnov, S. G. Ponomarev, A. S. Fionov, V. V. Kolesov, Ceramics International, 45 (2019) 23050-23060
- [17] M. C. de Andrade, G. N. Carneiro, E. L. Moreira, J. C. Araújo, V. C. A. Moraes, Materials Science Forum, 802 (2014) 285-290
- [18] T. Badapanda & V. Senthil & S. Panigrahi & Shahid Anwar, (2013), J Electroceram DOI 10.1007/s10832-013-9808-x
- [19] S. Bisen, M. Khan, A. Mishra, Journal of Materials Science: Materials in Electronics 31(2020)1-12
- [20] K. Madhan, R. Thiyagarajan, C. Jagadeeshwaran, et al. J Sol-Gel Sci Technol, 88 (2018) 584–592.
- [21] M. Al-Hilli, Iraqi Journal of Science 59(1A) (2018) 97-105
- [22] Q. Xu, Z. Li, Processing and Application of Ceramics, 14 (2020)188-194
- [23] W. Li, Z. Xu, R. Chu, P. Fu, G. Zang, Braz. J. Phys. 40(3), (2010) 353–356
- [24] A. K. Jonscher, J. Mater. Sci. Aug. 16(8) (1981) 2037–2060
- [25] P. Sateesh, J. Omprakash, G. S. Kumar, G. Prasad, J. Adv. Dielectr. 5 (2015) 1–13
- [26] S. Akter, A. Ahad, M. K. Das et. al. Materials Chemistry and Physics, 275 (2022) 125241
- [27] S. Mahajan, O. P. Thakur, C. Prakash, et al. Bull Mater Sci 34 (2011)1483–1489
- [28] H. Sharma, R. K. Kotnala, J. Shah, N. S. Negi, Results in Physics, 13 (2019) 102190
- [29] U. Younas, M. Atif, A. Anjum, M. Nadeem, T. Ali, R. Shaheen, W. Khalid and Z. Ali, RSC Adv. 13 (2023) 5293-5306
- [30] G. A. Kaur, S. Kumar, V. Sharma et.al. Inorganic Chemistry Communications, 151 (2023), 110644
- [31] D.C. Sinclair, A.R. West, J. Appl. Phys. 66 (1989) 3850–3856
- [32] D. Hassan, M. K. Mohammed and A. Hashim, World Journal of Advanced Research and Reviews, 19(03) (2023) 954–963
- [33] A. A. Shah and A. Azam, IOP Conf. Series: Materials Science and Engineering 577 (2019) 012089

